UNITED STATES OF AMERICA
NUCLEAR REGULATORY COMMISSION

ATOMIC SAFETY AND LICENSING BOARD

In the Matter of NEXTERA ENERGY SEABROOK, LLC (Seabrook Station, Unit 1)	Docket No. 50-443-LA-2 ASLBP No. 17-953-02-LA-BD01

Hearing Exhibit

Exhibit Number: NER064

Exhibit Title: Mohammed et al., "ASR Expansion of Concrete Beams with Various Restrained Conditions—612 Days of Accelerated Marine Exposure," Proceedings of the 12th International Conference on Alkali-Aggregate Reaction in Concrete 1169 (2004)

ASR EXPANSION OF CONCRETE BEAMS WITH VARIOUS RESTRAINED CONDITIONS – 612 DAYS OF ACCELERATED MARINE EXPOSURE

Tarek Uddin Mohammed*, Hidenori Hamada, Toru Yamaji, and Hiroshi Yokota
Port and Airport Research Institute
3-1-1 Nagase, Yokosuka shi, Japan 239-0826.

ABSTRACT

A detailed experimental investigation was carried out to understand alkali-silica reaction (ASR) induced expansion of concrete beams with various restrained conditions as well as the change in mechanical properties of concrete with the progress of ASR. For this, beam specimens of size $250 \times 250 \times 600$ mm and cylinder specimens of diameter 100 mm and length 200 mm were made with and without reactive aggregates. Additional NaOH was added to raise the total Na_2O equivalent alkali content to 6 kg/m^3 in concrete. Beam specimens were made with and without reinforcements. Various restrained conditions by the reinforcement were provided. The specimens were submerged in seawater of temperature 40°C. The investigation was carried out for 612 days of exposure. Lateral and longitudinal surface strains over the specimens were measured frequently. Strain gages were fastened with the steel bars before casting concrete and the strains were measured through a data logger once a day automatically till the age of 612 days exposure.

Young's modulus of concrete drops significantly due to ASR immediately after cracking, but later stabilizes. No remarkable difference in Young's modulus of concrete is found between the specimens cored from the ASR affected beams and the cylinder specimens subjected to direct exposure. The reduction of compressive strength was not as significant as Young's modulus. Internal restraint provided by the steel bars results in the reduction of surface strain in the restraint direction. The degree of restraint has a significant influence on the surface strain as well as strain, i.e. ASR induced stress in the bars. Linear relationships between the surface strain and the strain over the steel bars for various restrained conditions in concrete are found, especially for the cases with highly restrained conditions. The expansion process is divided into three remarkable periods, such as incubation period, cracking period, and stabilized period.

Keywords: Alkali-silica reaction, Concrete, Steel bar, Strain.

1 INTRODUCTION

Alkali-silica reaction (ASR) occurs between the reactive silica in aggregate and the alkali solution in concrete. The reaction produces a gel that absorbs water and consequently expands. The gel is first restrained to spread freely into concrete. As a result, tensile stress is built up locally and cracking occurs when the pressure generated at localized sites of expansive reaction exceeds the tensile strength of concrete. ASR related studies were carried out since 1940 covering a wide scope related to this problem [1~17]. Nevertheless, detailed studies on the strain induced over the concrete surface as well as the steel bars with various restrained conditions provided by the embedded steel bars inside concrete are still necessary.

With the above-mentioned background, a detailed experimental study was carried out on plain and reinforced concrete beams of size $250 \times 250 \times 600$ mm to investigate the ASR induced surface strain over the concrete surface as well as the strains over the steel bars embedded in concrete. Moreover, cylinder specimens were also investigated for the evaluation of variations in pulse velocity, compressive strength, and Young's modulus of concrete with the progress of ASR. The study was continued until 612 days. Intermediate reports of this investigation were reported at 197 days and 383 days of exposure [18,19]. In this report, the key results till the age of 612 days of exposure are summarized.

After 612 days of exposure, the remaining specimens were transferred to the marine splash zone for further monitoring of the specimens.

2 EXPERIMENTAL METHOD

2.1 Materials

Ordinary portland cement (OPC) was used. The physical properties and chemical analysis are shown in **Table 1**. Additional NaOH was added to raise the Na_2O equivalent alkali content in concrete to 6 kg/m^3.

Crushed reactive (chert) and non-reactive (granite) coarse aggregates were used. The sand was non reactive. The properties of reactive and non-reactive aggregates are shown in **Table 2**. The reactivity of the coarse aggregates was confirmed by concrete prism tests before making the specimens as per ASTM C1293. Japanese Industrial Standard round (SR295) and deformed (SD295A) steel bars were used. The mechanical properties of the steel bars are listed in **Table 3**. The size of the end steel plates was $50 \times 50 \times 6$ mm (SS 400). The end plates were rigidly welded with the steel bars.

Table 1 Properties of Cement

Density (kg/m^3)	3160
Blaine Fineness, cm^2/g	3190
Ignition Loss, %	0.7
SiO_2, %	21.3
Al_2O_3, %	5.3
CaO, %	64.4
MgO, %	2.2
SO_3, %	1.9
Fe_2O_3, %	2.6
Na_2O Equiv., %	0.65

Table 2 Properties of the Aggregates

Aggregate	Density (kg/m^3)	Water Absorp.(%)	FM
Reactive Coarse Aggre.	2630	0.62	6.61
Non-React. Coarse Aggre.	2640	0.76	6.67
Fine Aggre.	2600	2.32	2.91

Table 3 Mechanical Properties of the Steel Bars

Items	R-13mm	D-12.7 mm	R-25 mm	R-6 mm
Yield Strength (MPa)	373	387	370	299
Young's Mod. ($\times 10^5$ MPa)	2.03	1.80	2.11	1.96
Yield Strain ($\mu\varepsilon$)	1837	2150	1750	1525
Ultimate Strength (MPa)	547	565	561	489
Elongation (%)	23	20	25	21

R-Round Bar, D-Deformed Bar

Table 4 Mixture Proportions of Concrete

	Normal Concrete	ASR Concrete
G_{max} (mm)	20	20
Slump (cm)	11±1	11±1
Air (%)	4±1	4±1
W/C (%)	47	47
s/a (%)	41	41
W (kg/m^3)	170	170
C (kg/m^3)	362	362
S (kg/m^3)	720	720
G (kg/m^3)	1051	1047
AEWRA(kg/m^3)	0.905	0.905
AEA (g/m^3)	3.62	3.62
NaOH (kg/m^3)	-	4.7

W, C, G, and S refer respectively to water, cement, gravel and sand. s/a is the sand-aggregate ratio. AEA and AEWRA mean air-entraining, and air-entraining water-reducing admixtures, respectively.

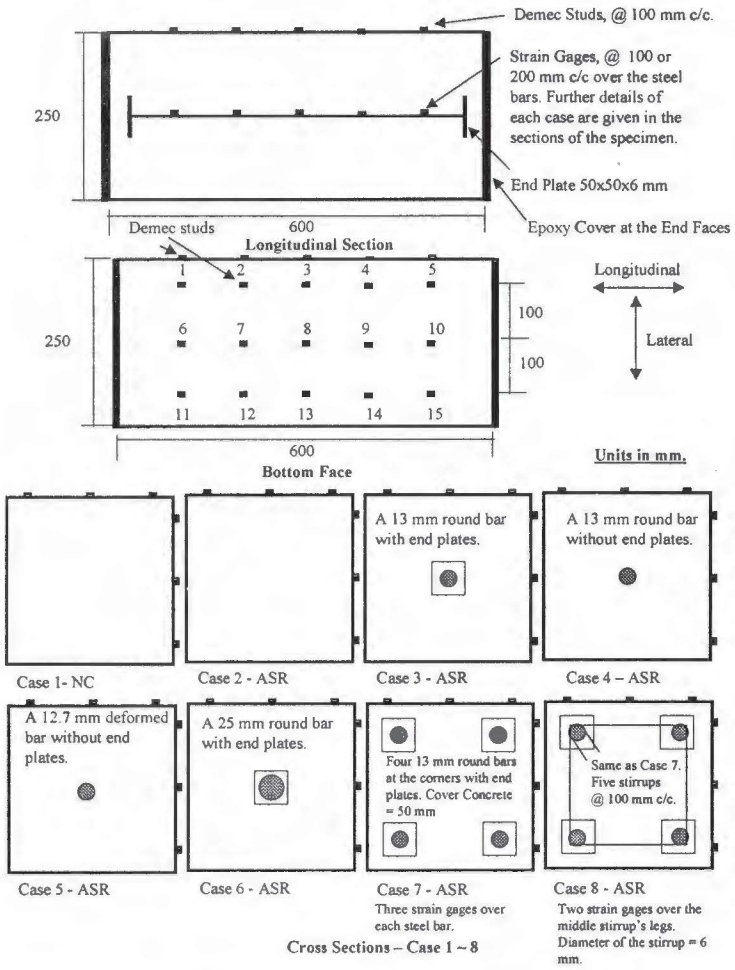

Fig. 1 Layout of the Specimens

Table 5 Physical Properties and Chemical Composition of Seawater

Density (kg/m^3)	pH	Na ppm	K ppm	Ca ppm	Mg ppm	Cl ppm	SO_4 ppm	CO_3 ppm
1022	7.77	9290	346	356	1167	17087	2378	110

Type FLA-3-11-5LT and Type FLK-2-11-5LT strain gauges were used to measure strain over the main steel bars and stirrups, respectively.

2.2 Mixture Proportion

Mixture proportions of concrete are summarized in **Table 4**. W/C was 0.47. The slump of the fresh concrete was 11±1 cm and air content 4±1 %. Both air entraining and air entraining water reducing agents were used. Mixing water was tap water.

2.3 Specimens and Method of Evaluations

Plain and reinforced concrete beam specimens of size $250 \times 250 \times 600$ mm were made as shown in **Fig. 1** with and without reactive coarse aggregates. Eight cases were made. The cross sections of all cases are given in **Fig. 1**. A brief explanation of the cases investigated in this study is given below:

Case1 Normal concrete (made with non-reactive aggregate) without reinforcement.

Case 2 ASR Concrete without reinforcement.

Case 3 ASR concrete. A 13 mm round bar was embedded at the center with end plates.

Case 4 ASR concrete. A 13 mm round bar was embedded at the center without end plates.

Case 5 ASR concrete. A 12.7 mm deformed bar was embedded at the center without end plates.

Case 6 ASR concrete. A 25 mm round bar was embedded at the center with end plates.

Case 7 ASR concrete. Four 13 mm round bars were embedded at the corners with end plates.

Case 8 ASR concrete. Four 13 mm round bars were embedded at the corners with end plates. In addition, five stirrups (round bar, 6 mm diameter) were embedded @ 100 mm c/c.

The end plates were used to simulate the effect of the bar with end anchorage. The presence of end plates also confines the concrete surrounding the steel bars enclosed by the end plates. Therefore it is expected that for these cases (Case 3, Cases 6~8), the influence of type of bars (plain or deformed) will be negligible.

For Case 1, two specimens were made. For all other cases, three specimens per each case were made. Demec studs were placed over the concrete surface @ 100 mm c/c in both lateral and longitudinal directions (**Fig. 1**). They were placed on the bottom face (opposite to the finishing face after casting concrete) and one side face of the specimens. Here, the results on the side face are only explained. Five strain gages were fastened over the steel bars @ 100 mm c/c in Cases 3~6. In Cases 7 and 8, three strain gages were fastened @ 200 mm c/c over each steel bar. In Case 8, in addition to strain gages over longitudinal steel bars, two strain gages were fastened over the mid stirrup, one at the vertical leg and one at the horizontal leg. To fasten the strain gauge, a smooth surface was prepared over the steel bars and the strain gauges were glued over it and covered with adhesive tape. All strain gages were connected with a data logger. Two switch boxes were also connected with the data logger for the automatic recording of all strains (total 138 locations) over the steel bars concurrently once in a day.

After 28 days of standard curing, the demec studs were fastened over the concrete surface and at the age of about 45 days the specimens were transferred to the exposure tanks. Three wooden tanks were specially fabricated for this purpose. The specimens were rested on three plastic pipes (diameter 3 cm) glued over the bottom face of the tank. This was done to reduce the friction at the contact surfaces. The specimens were submerged in seawater directly supplied from the sea. The physical properties and chemical composition of seawater are listed in **Table 5**. The temperature of seawater was controlled at around 40°C. One heater was placed in each tank and the water was continuously circulated through a pump to maintain a uniform temperature in the tank. The tanks were covered during exposure.

Strain over the steel bars was measured once in a day through the data logger automatically. Some of the strain gages became inactive after cracking of the specimens. The average of all strain measured over the steel bars for each specimen is reported as the representative strain for the specimen. The change in length between the demec studs was measured by a digital extensometer periodically. The side face with demec studs was maintained at the top in the tank for easy measurements of length change during exposure. The average of all measured longitudinal strains is defined as longitudinal strain for each specimen. In the same way, the average of all lateral strains is defined as the lateral strain. Cracks were marked over the specimens periodically and photographs were taken. Large crack widths were also measured. The measurements were taken just after removing a portion of water from the tank so that the measurement of length between the demec studs is possible. The tank was filled and covered soon after all measurements, such as change in length between the demec studs, recording of the large crack widths and marking the cracks, and taking photographs.

In addition to the prism specimens, cylinder specimens (12 specimens with non-reactive aggregate and 36 specimens with reactive aggregate) 100 mm in diameter and 200 mm in length were also made. The specimens were exposed in the tank with the prism specimens. The specimens were periodically tested for pulse velocity, compressive strength, and Young's modulus. Before measurements, the specimens to be tested were transferred in a controlled room of temperature about 20°C and relative humidity of more than 80%. The specimens were also kept covered with wet cloths to prevent moisture loss.

After 303 days of continuous exposure, one specimen from each case (Cases 2~8) was cut to collect the steel bars as well as to see the internal condition of the specimens, the crack depths, and corrosion over the steel bars. In addition, samples were also carefully collected to measure the porosity of the mortar portions at the inner and outer regions, SEM evaluation of the dense matrix, porous matrix, and entrained air voids. Mechanical properties of the steel bars were also tested. These data were reported in Reference [19]. The exposure of the remaining specimens was continued till the age of 612 days. The specimens were transferred to the marine splash zone at 612 days of exposure to monitor the further expansion of the specimens. Monitoring of the surface strain and evaluation of the mechanical properties of concrete are continuing.

3 EXPERIMENTAL RESULTS AND DISCUSSION

The results of this study are explained in the following subsections:

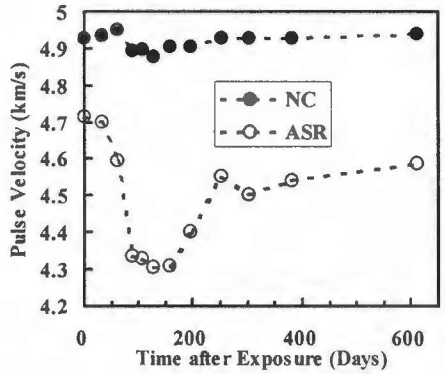

Fig. 2 Pulse Velocity (Cylinder Specimens)

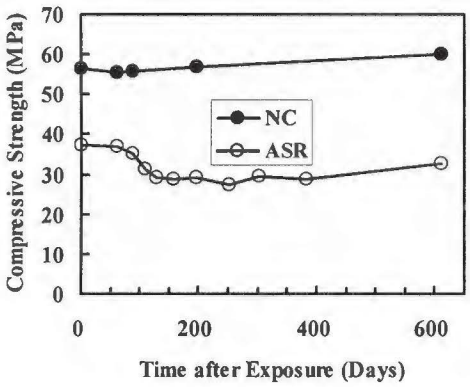

Fig. 3 Compressive Strength (Cylinder Specimens)

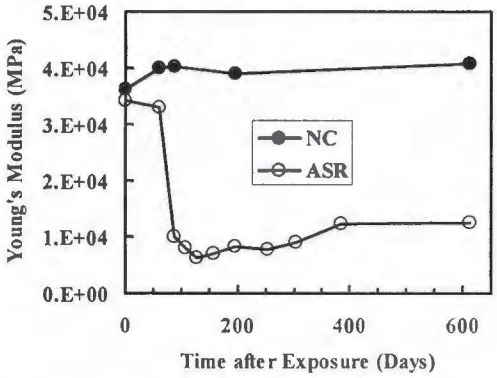

Fig. 4 Young's Modulus (Cylinder Specimens)

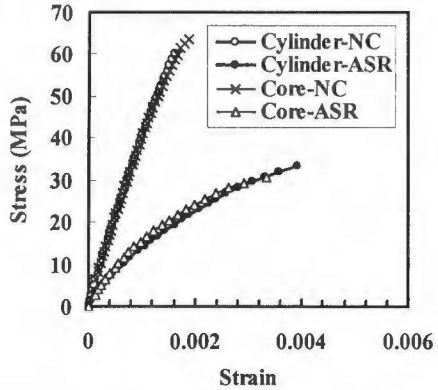

Fig. 5 Stress-Strain Curves (Core and Cylinder)

3.1 Pulse Velocity, Compressive Strength and Young's Modulus

The variations of the ultrasonic pulse velocity, compressive strength, and Young's modulus with the exposure period are shown in **Figs. 2~4**. The pulse velocity decreases gradually during the early age of exposure. It quickly drops after cracking at around 65 days of exposure. Later it increases slightly and reaches a constant value without decreasing further due to the healing of voids and cracks by ASR gel. The compressive strength is slightly reduced at the early age of exposure. The reduction is relatively more immediate after cracking at 65 days of exposure. However, no significant reduction is observed later, i.e., a stable value is reached. The lower strength of ASR specimens compared to the specimens made with non-reactive aggregate cannot be explained here, as no specimens were tested for normal concrete with the additional alkali. The Young's modulus gradually decreases at early age of exposure and quickly drops after cracking, and finally becomes almost stable. The change in Young's modulus is more significant than any other changes explained earlier, such as pulse velocity and compressive strength. The significant reduction in Young's modulus of concrete due to ASR at the early age of exposure was also reported by Fournier and Berube [4] and Mohammed et al. [18,19] being attributed to the generation of micro cracking in concrete due to the ASR. Typical stress-strain curves of the cylinder and cored cylinder specimens from the beams are shown in **Fig. 5** at the exposure period of 612 days. No significant difference is found between the cored and cylinder specimens for normal concrete and ASR concrete.

From the above-mentioned results till the age of 612 days, ASR induced expansion is divided into three periods: the incubation period, cracking period, and stabilized period. In the incubation period, the change in properties is slow, in the cracking period the change is fast, and in the stabilized period no significant change is found. The same process of expansion was also mentioned in another study [5].

3.2 Longitudinal and Lateral Strains Over the Concrete Surface

Longitudinal (ε_{lo}) and lateral (ε_{la}) strains over the specimens were calculated based on the measured surface strains over the specimens by using the following equations:

$$\varepsilon_{lo} = \frac{\sum_{i=1}^{4}\varepsilon_{i,i+1} + \sum_{i=6}^{9}\varepsilon_{i,i+1} + \sum_{i=11}^{14}\varepsilon_{i,i+1}}{12} \quad (1)$$

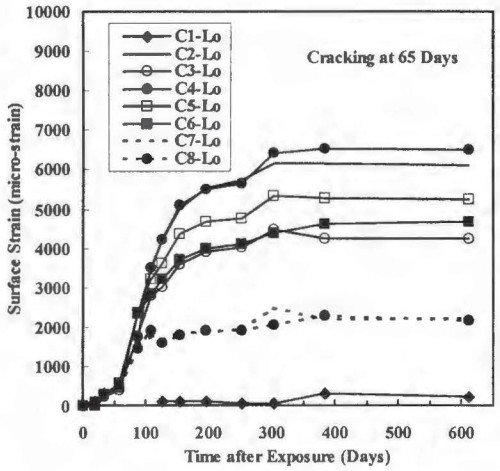

Fig. 6 Longitudinal Surface Strain

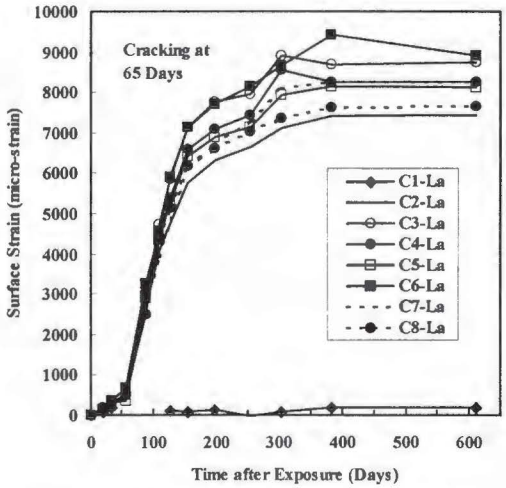

Fig. 7 Lateral Surface Strain

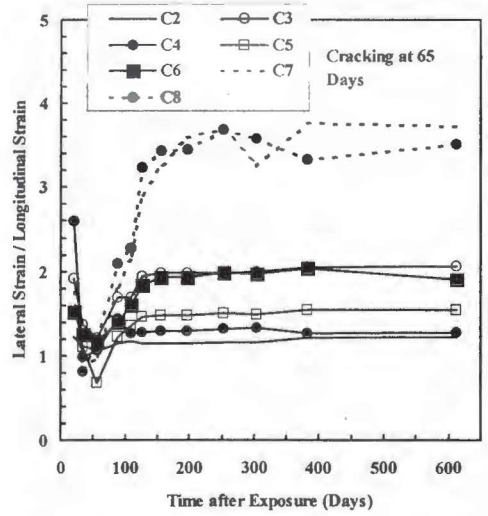

Fig. 8 Ratio of Longitudinal to Later Surface Strain (Lo/La)

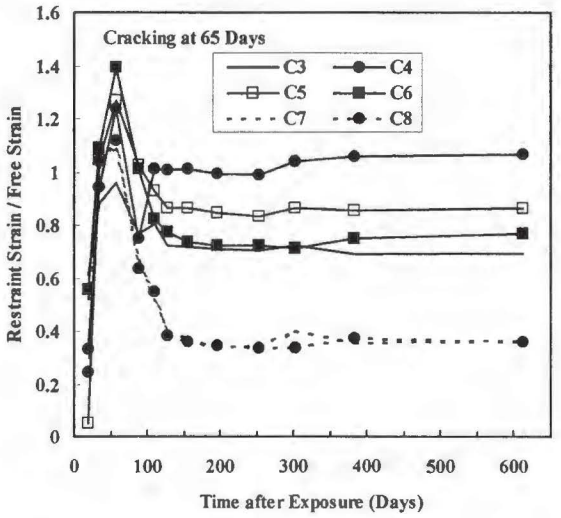

Fig. 9 Restrained Surface Strain (Cases 3~8) Normalized by Free Surface Strain (Case 2)

$$\varepsilon_{la} = \frac{\sum_{i=1}^{10} \varepsilon_{i,i+5}}{10} \quad (2)$$

Where, $\varepsilon_{i,j}$ is strain between studs i and j (**Fig. 1**). The longitudinal and lateral strains over the specimens for all cases are shown in **Figs. 6 and 7**. The ratios of lateral to longitudinal surface strain are shown in **Fig. 8**. For Case 1, the surface strain was lower than 200 $\mu\varepsilon$ after 612 days of exposure and also no cracks were found over the specimens. The results of each individual specimen of each case until the age of 198 days were reported in an intermediate report [18]. The dispersion of data among the specimens of each case was very small. Irrespective of the cases, no significant difference in strain is observed at the early stage of exposure. However, after cracking at 65 days of exposure, a significant difference in longitudinal strain is observed depending on the restraint provided by the steel bars inside the specimens. Irrespective of the cases, it is also found that strain increases gradually and becomes almost stable later. The strain over the specimens for Cases 3~8 were normalized by the free strain over the steel bars (Case 2). The results are shown in **Fig. 9**. The key results of expansion related to each individual cases (Cases 2~8) are explained below:

Case 2

This is the ASR case without reinforcement. A significant amount of lateral and longitudinal strains

is observed (**Figs. 6 and 7**). The longitudinal strain stabilizes at about 6000 $\mu\varepsilon$ (0.6%). The lateral strain stabilizes at around 7000 $\mu\varepsilon$ (0.7%). As no steel bar was embedded in this case, therefore, the specimens were free to expand in both lateral and longitudinal directions. The ratio of the lateral to longitudinal strains is close to unity, indicating almost equal strain in lateral and longitudinal directions (**Fig. 8**).

Case 3

This is the ASR case with a 13 mm steel bar at the center with end plates. A clear difference between the longitudinal and lateral strains is observed after cracking of the specimens. The restraint in the longitudinal direction provided by the steel bars with end plates reduces the surface strain over the specimens in the longitudinal direction. The lateral and longitudinal strains are around 9000 and 4000 $\mu\varepsilon$, respectively after 612 days of exposure. The ratio of the lateral to longitudinal strains almost stabilized at around 2. The restraint strain of this case was about 70% of the free strain of Case 2 (**Fig. 9**). Comparing Cases 2 and 3, the change in the strains due to the restraint can be clearly realized after cracking of the specimens.

Case 4

In this ASR case, a 13 mm round bar was embedded at the center of the specimen without end plates. Removal of the end plates from the end of the bar reduces the degree of restraint in the longitudinal direction compared to Case 3. The strains in the lateral and longitudinal directions become about 8000 $\mu\varepsilon$ and 6500 $\mu\varepsilon$, respectively after 612 days of exposure. The restraint strain was similar to the free strain of Case 2 (**Fig. 9**). The results indicate that a little restraint is provided by the embedded steel bar for Case 4. The ratio of the lateral to longitudinal strains stabilizes at around 1.3 (**Fig. 8**). The higher value of lateral to longitudinal strain at the early age of exposure is presumably due to the error in measurements of a very small strain over the specimen.

Case 5

In this ASR case, to increase the degree of restraint compared to Case 4, a deformed bar of diameter 12.7 mm was embedded at the center of the specimens. The lateral and longitudinal strains become 5500 $\mu\varepsilon$ and 8000 $\mu\varepsilon$, respectively. As in the above cases, the longitudinal restraint provided by the steel bar in concrete results in the reduction in longitudinal strains compared to the lateral strains. However, this reduction is more than Case 4, i.e. the case with a plain bar without end plates, but less than Case 3, i.e., the case with a plain bar with plates at the ends. In Case 5, the degree of restraint is higher compared to Case 4, but lower compared to Case 3. The restraint strain is 85% of the free strain of Case 2 (**Fig. 9**). The results strongly suggest that the degree of the restraint has a significant influence on the strain over the concrete surface. The ratio of the lateral to longitudinal strains stabilizes at around 1.5, which is higher than Cases 2 and 4, but lower than Case 3 (**Fig. 8**).

Case 6

In this ASR case, a 25 mm bar was embedded at the center with end plates. The steel area is about 3.7 times higher than Case 3. After cracking of the specimens, a clear difference between the lateral and longitudinal strains is observed as in Case 3. No remarkable difference between the lateral and longitudinal strains is observed between Case 6 and Case 3. The ratio of the lateral to longitudinal strain stabilizes at around 1.9, which is slightly lower than Case 3 (**Fig. 8**). No significant difference in the surface strains of Case 3 and Case 6 indicates that both are providing the same amount of restraint. The restraint strain is 75% of the free strain, which is 70% for Case 3 (**Fig. 9**). However, strain over the steel bars was lower for Case 6 compared to Case 3. These data are explained later.

Case 7

In this ASR case, four 13 mm steel bars were provided with end plates. The total area of the steel bar was similar to Case 6. For Case 7, a significant reduction in the longitudinal strains is observed compared to the other cases explained above. The longitudinal and lateral strains after 612 vdays of exposure are 2000 $\mu\varepsilon$ and 8000 $\mu\varepsilon$, respectively. The results indicate that the position of the steel bars in the specimens has a significant influence on the surface strains. The nearer the longitudinal steel bar to the concrete surface, the lesser the longitudinal strain. The ratio of the lateral to longitudinal strain stabilizes at around 4, which is the highest compared to the other cases explained above (**Fig. 8**). The restraint strain is about 35% of the free strain (**Fig. 9**).

Case 8

In this ASR case, in addition to the four corner reinforcements as in Case 7, five stirrups (6 mm diameter) were embedded in the specimens to limit the lateral strains. Compared to Case 7, a slight reduction in lateral strain is observed. However, the

longitudinal strain is almost the same as Case 7. The ratio of the lateral to longitudinal strain stabilizes at around 3.4, which is lower than Case 7 (**Fig. 8**). The restraint strain is 35% of the free strain, the same as Case 7 (**Fig. 9**).

From the surface strain data of ASR specimens, it is clearly realized that before cracking the rate of expansion is slow, and after cracking it increased rapidly, and finally almost stabilized. Almost no difference in strain is observed after about 400 days of exposure. From these results, the expansion process is divided into incubation period with a slow rate of expansion, cracking period with a rapid rate of expansion, and finally a stabilized period without any significant expansion. Pulse velocity, compressive strength, and Young's modulus data also show the same trend as explained in the previous subsection. The same process of strain development over the steel bars in concrete is also observed. These data are explained in the next subsection.

3.3 Strain Over the Steel Bars Embedded in Concrete

Average strain over the steel bar in each specimen is explained in this subsection. Cases 1 and 2 were made without reinforcement, therefore, the explanation begins from Case 3. The average strain over the steel bar for each case is shown in **Fig. 10.** The average strain of a specimen represents the average strains obtained from the strain gages embedded in each specimen (5 gages for each specimen for Cases 3~6, and 12 gages for each specimen for Cases 7 and 8). The average strain of each case represents the average strain of three specimens. For Case 8, two strain gages were also fastened over the mid stirrup, one on the vertical leg and one on the horizontal leg. The average strain of these strain gages is defined as the average strain over the stirrup of a specimen. Again, average strain of three specimens means average strain over the stirrup of Case 8.

Case 3

After cracking at around 65 days, the strain over the steel bars quickly increases and stabilizes at around 1500 $\mu\varepsilon$ for a certain period and then decreased to the level of 1200 $\mu\varepsilon$. The reduction of the strain over the steel bar cannot be explained. However, it is presumably due to the leaching of the alkali-silica gel from concrete, and therefore reducing the force induced by the expansion. Relevant data on this matter are explained in Reference [19].

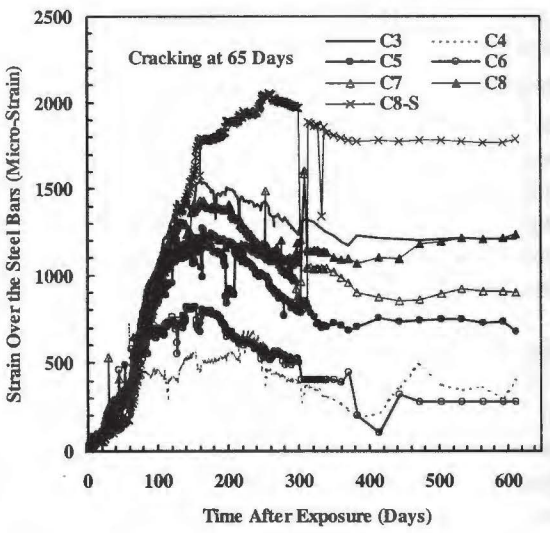

Fig. 10 Strain Over the Steel Bars

Case 4

The strain over the steel bars decreases dramatically compared to Case 3. It stabilizes at around 500 $\mu\varepsilon$ for a certain period and later decreases as in Case 3. The results indicate that with the absence of the end plates, the degree of restraint provided by the steel bars in concrete decreases and concrete is allowed to expand more freely.

Case 5

The strain over the steel bars stabilizes at around 1250 $\mu\varepsilon$ for a certain period, which is lower than Case 3, but higher than Case 4. It is supposed due to the greater restraint provided by the deformation over the deformed bar compared to Case 4 with plain bar. The degree of restraint for Case 5 will be less than Case 3 with end plates. The results strongly indicate that ASR induced strains will depend on the restraint provided by the steel bars in concrete.

Case 6

The strain over the steel bars stabilizes at around 750 $\mu\varepsilon$ for a certain period, which is about half of the stabilized strain of Case 3. The steel area in Case 6 was about 3.7 times higher than Case 3, however the strain over the steel bar for Case 6 is about half of Case 3. No significant difference in the surface strains is observed with the variation of the amount of the steel bars as explained in the previous section (**Figs. 6 and 7**). It is supposed due to the lower restraint provided by the end plates of Case 6. The size of the end plates for Cases 3 and 6 was the same but the diameter of the bar was double that of Case 6 compared to Case 3. It is important to note that a 25 mm round bar was not available in the market,

therefore, larger deformed bars were polished to make 25 mm round bars. Compared to Case 3, the large diameter of Case 6 leads to a relatively smaller area at the ends to provide the restraint. It is expected that the smooth steel surface as well as less effective plate area at the ends of the bar result in less restraint against expansion.

Case 7

The strain over the steel bars stabilized at around 1400 $\mu\varepsilon$ for a certain period. The amount was almost the same as the Case 3, where only one steel bar was embedded at the center with end plates. It is also important to note that in Case 7, the total amount of longitudinal steel area was kept similar to Case 6. However, the strain over the steel bars was higher for Case 7 compared to Case 6. The surface strain was already discussed in the previous section. The results strongly support the influence of the location of the steel bars on the strain development over the bar, and also over the surface as explained before. The strain over the bar near the surface is higher than the bar far from the surface.

Case 8

Compared to Case 7 no significant change in the strain over the steel bars is observed with the addition of the stirrups in the specimens.

The strain over the legs of the stirrup (C8-S) is higher than the longitudinal strain over the main steel bars. The strain over the stirrup becomes 2000 $\mu\varepsilon$ after 383 days of exposure, which is higher than the yield strain of the steel bars. Relatively higher lateral surface strain compared to the longitudinal surface strain leads to the generation of higher strain over the stirrup.

From the results explained in this subsection, it is understood that the strain over the steel bars increases slowly at the early age of exposure, then rapidly increases after cracking and finally stabilizes for a certain period. Therefore, it is clear that the strain development over the steel bars closely follows the three stages of ASR expansion i.e., the incubation period, the cracking period, and the stabilized period as explained earlier. It is also important to note that a reduction in strain over the steel bars is observed after a certain stabilized period, which is presumably due to the leaching of ASR gel from the specimens. For large specimens, and also specimens not exposed to seawater, this phenomenon may not be observed. Therefore, it is recommended to carry out additional investigation on large cube specimens. Relevant data on the leaching of gel were explained in Reference [19]. Slip over the steel bars may also influence the results.

3.3 Crack Maps, Crack Intensity, Crack Widths and Depths, and Overall Volume Expansion

Crack maps over the specimens is shown in **Fig. 11**. No new cracks were developed from 383 to 612 days of exposure. Fewer lateral cracks are observed for Cases 7 and 8. It is expected due to the placement of the steel bars near the surface of the specimens. A significant amount of strain in the lateral direction causes the cracks to run mostly in the longitudinal direction for Cases 7 and 8. No significant difference in the crack patterns is observed in other cases. At 612 days, the data related to the crack intensity, crack widths and depths were similar to the exposure at 383 days, which were explained in Reference [19]. A summary of these results is provided here. Crack intensity is defined as the number of cracks per unit cm of the specimens in the lateral or longitudinal direction. It was found that crack intensity increased rapidly at the beginning of the cracking and later no significant difference was found. The crack intensity in the longitudinal direction was lower for Cases 7 and 8 compared to the others. It is due to the significant amount of restraint provided by the steel bars at the corners of the beams. A tendency of higher crack intensities in the lateral direction was found for Cases 7 and 8. It is presumably due to the significant amount of strain in the lateral direction, which helps to generate the cracks in the longitudinal direction.

The change in the crack widths was observed in the cracking period with the development of a few additional new cracks. The crack width was stabilized later. New cracks were not developed in the stabilized period. Relatively lower crack widths were observed for Cases 7 and 8. Crack widths (lateral direction) and depths in the longitudinal directions were measured after cutting the specimens in the longitudinal directions. No difference in the average crack widths is observed between Case 3, 6, 7, and 8. Relatively wider cracks were observed for Cases 2, 4, and 5. No steel bars are provided in Case 2, therefore it is free to expand, which causes the generation of wider cracks. The less restraint provided by the steel bars for Cases 4 and 5 also results in wider cracks. Relatively larger crack depths were also observed for the cases with wider crack widths. The depths of the surface cracks were limited over a thin surface region surrounding the specimens. For this reason, the chloride penetration is also limited to the surface region. The volume expansion was reduced with the improvement of restraint conditions.

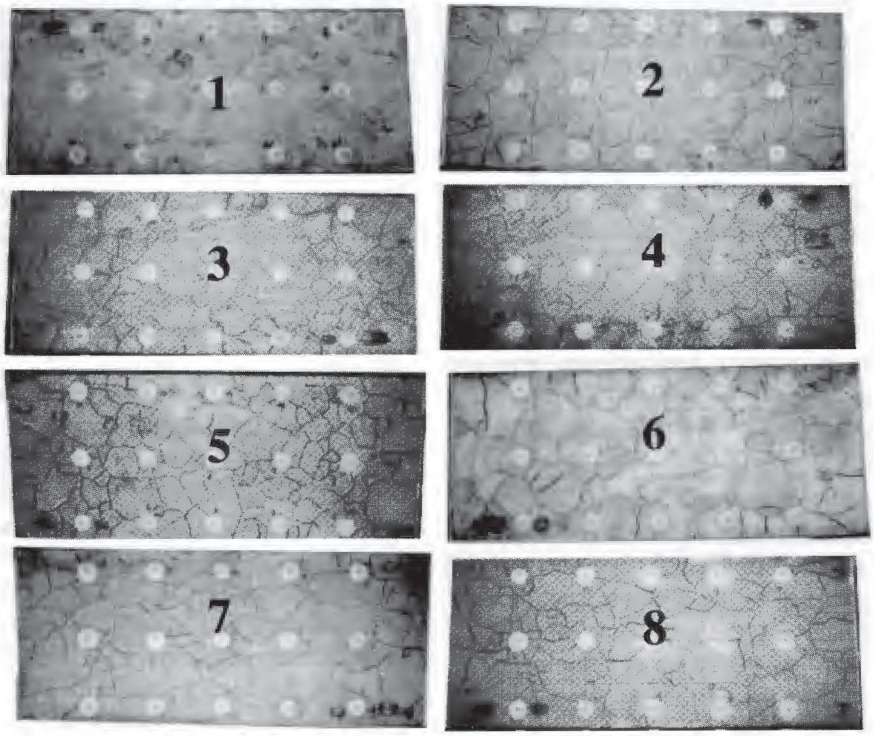

At 383 Days of Exposure

Fig. 11 Crack Maps Over the Specimens

Table 6 The Value of β

Case	The value of β
3	0.42
4	0.11
5	0.27
6	0.14
7	0.71
8	0.60
8 (Stirrup)	0.26

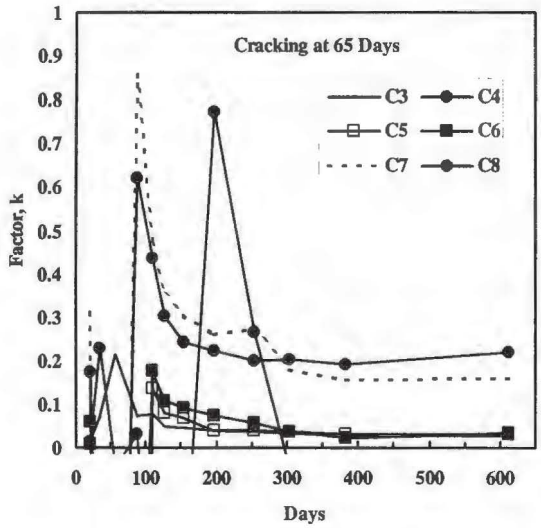

Fig. 12 Factor k for Different Cases

3.5 Relationship Between Surface Strain and Strain Over the Steel Bars

To predict the relationships between the surface strain and the strain over the steel bars, the data until the age of 198 days were used. After 198 days, in many cases it was found that the strain over the steel bars decreased. Inclusion of these data causes a poor relation between the surface strain and strain over the steel bars. The relationship between the surface strain and strain over the embedded steel bars is proposed by the following linear relationship [19]:

$$\varepsilon_{st} = \beta \varepsilon_{con} \tag{3}$$

The factor β depends on the internal restraint provided by the steel bars inside the specimens as well as the location of the bars inside the specimens. The values of β for different cases are summarized in **Table 6**.

For Case 4, a significant amount of slip over the steel bars causes a poor linear relationship [19]. For Cases 5 and 6, the relationship also becomes relatively poor for the same reason. Generally, the correlations were good for highly restrained cases (The R^2 value was more than 0.95 [19])). The value of β is generally higher for the higher restrained cases (Cases 3, 7, and 8).

3.6 Calculation for the Effective Area Balancing Compressive Stress And Tensile Stress of Concrete

The following notation are assumed to calculate the tensile force in the steel bar and the compressive force in concrete:

ε_f = Free Expansion (Case 2)

ε_r = Strain at Restrained Condition (Cases 3~8)

F_c = Compressive Force in Concrete

F_s = Tensile Force in Steel

E_c = Young's Modulus of Concrete

E_s = Young's Modulus of Steel Bar

A_c = Area of Concrete

A_s = Area of Steel Bar

k = Factor to convert total area of concrete to the effective area

No restraint against expansion is provided for Case 2 (**Fig. 1**). Different restrained conditions were provided for Cases 3 ~ 8. The difference in strain for the restrained cases (Cases 3~8) and restrained free case (Case 2) is expected to be developed with the presence of a free stressing force in the steel bars for Cases 3~8.

Compressive force in concrete can be calculated by the following equation based on the abovementioned notations:

$$F_c = kA_cE_c(\varepsilon_f - \varepsilon_r) \quad (4)$$

Tensile force in the steel bars can be calculated by using the following equation:

$$F_s = A_sE_s\varepsilon_s \quad (5)$$

Equating tensile force with compressive force, the factor, k can be calculated by using the following equation:

$$k = \frac{A_s}{A_c}\frac{E_s}{E_c}\left(\frac{\varepsilon_s}{\varepsilon_f - \varepsilon_r}\right) \quad (6)$$

Replacing Es (**Table 3**), Ec (**Fig. 3**), ε_f (**Fig. 6**), ε_r (**Fig. 6**), ε_s (**Fig. 10**), and other variables (A_s and A_c), the value of "k" can be calculated as shown in **Fig. 12**. The value of "k" varies with the restrained conditions. A higher value of k indicates a larger effective area of concrete is necessary to valance the induced stress in steel bars due to ASR.

3.7 Remaining Studies

Investigations are still continuing on the surface strain of the specimens at the marine splash exposure. Unfortunately, all strain gages became inactive and therefore monitoring of the strain over the steel bars was stopped. The surface strain data of the splash exposure zone will be summarized after couple of years of exposure.

4 CONCLUSIONS

Based on the scope of this study, the following conclusions are drawn:

1. Young's modulus of concrete drops significantly due to ASR immediately after cracking, but later stabilizes. No remarkable difference in Young's modulus of concrete is found between the specimens cored from the ASR affected beams and the cylinder specimens subjected to direct exposure. The reduction of compressive strength was not as significant as Young's modulus.
2. Internal restraint provided by the steel bars results in the reduction of surface strain in the restraint direction. The degree of restraint has a significant influence on the surface strain as well as strain, i.e. ASR induced stress in the bars.
3. Linear relationships between the surface strain and the strain over the steel bars for various restrained conditions in concrete are found, especially for the cases with highly restrained conditions.
4. The expansion process is divided into three remarkable periods, such as incubation period, cracking period, and stabilized period.
5. For higher restraint condition, a larger effective area of concrete is necessary to valance the ASR-induced tensile force in the steel bar. The factors to calculate the effective area for various restrained conditions investigated here are provided.

ACKNOWLEDGEMENTS

The authors wish to express their gratitude and sincere appreciation to the authority of *Port and Airport Research Institute, Independent Administrative Institution, Japan* for giving support to perform this study. The authors are very thankful to Mr. Koji Horiguchi and Mr. Kazuyuki Godo of Chuken Consultant, Utsunomiya Technical Center, Japan for their kind help in preparing the specimens. The authors also thankful to Ms. Madoka Satoh of

Materials Division, Port and Airport Research Institute for her help during the experimental process.

REFERENCES

[1] Stanton, T.E., Expansion of Concrete Through Reaction Between Cement and Aggregate, Proceedings, ASCE, 1940, 66 (10), 1781-1811.

[2] Kammer, H.A., and Carlson, R.W., Investigation of Causes of Delayed Expansion of Concrete in Buck Hydroelectric Plant, ACI Journal, Proceedings, 1941, 37, 665-671.

[3] Hobbs, D.W., Alkali-Silica Reaction in Concrete, Thomas Telford Limited, London, 1988.

[4] Fournier, B., and Berube, M., Alkali-aggregate Reaction in Concrete: A Review of Basic Concepts and Engineering Implications, Canadian Journal of Civil Engineering, 2000, 27, 167-191.

[5] Shenfu, F., and Hanson, J. M., Length Expansion and Cracking of Plain and Reinforced Concrete Prisms Due to Alkali-Silica Reaction, ACI Materials Journal, 1998, 95 (4), 480-487.

[6] Zhang, C., Wang, A., Tang, M., Zhang, N., Influence of Dimension of Test Specimens on Alkali-Aggregate Reactive Expansion, ACI Materials Journal, 1999, 96 (2), 204-207.

[7] Prezzi, M., Monterio, P.J.M., and Sposito, G., Alkali-Silica Reaction – Part 2: The Effect of Chemical Admixtures, ACI Materials Journal, 1998, 95 (1), 3-10.

[8] Prezzi, M., Monterio, P.J.M., and Sposito, G., Alkali-Silica Reaction – Part I : Use of Double-Layer Theory to Explain the Behavior of the Reaction Product Gels, ACI Materials Journal, 1997, 94 (1), 10-17.

[9] RILEM, Aggregates for Alkali-Aggregate Reaction – International Assessment of Aggregates for Alkali-Aggregate Reactivity, TC 106-AAR, Materials and Structures, 2000, 33, 88-93.

[10] Ahmed, T., Burley, E., Rigden, S., The Static and Fatigue Strength of Reinforced Concrete Beams Affected by Alkali-Silica Reaction, ACI Materials Journal, 1998, 95 (4), 376-388.

[11] Ahmed, T., Burley, E., Rigden, S., Effect of Alkali-Silica Reaction on Bearing Capacity of Plain and Reinforced Concrete, ACI Structural Journal, 1999, 96 (4), 557-570.

[12] Ahmed, T., Burley, E., Rigden, S., Effect of Alkali-Silica Reaction on Tensile Bond Strength of Reinforcement in Concrete Tested under Static and Fatigue Loading, ACI Materials Journal, 1999, 96 (4), 419-428.

[13] Thaulow, N., Hjorth, U.J., and Clark B., Composition of Alkali Silica Gel and Ettringite in Concrete Railroad Ties: SEM-EDX and X-Ray Diffraction Analyses, Cement and Concrete Research, 1996, 26 (2), 309-318.

[14] Diamond, S., ASR – Another Look at Mechanisms." In Proceedings of the Eighth International Conference on Alkali Aggregate Reaction in Concrete, Kyoto, Japan, Ed. Okada, K., Nishibayashi, S., and Kawamura, M., 1989, 83-94.

[15] Kagimoto, H., Sato, M., and Kawamura, M, Evaluation of Degree of ASR Deterioration in Concrete and Analysis of Pore Solutions." Concrete Library of JSCE, 2000, 36, 281-293.

[16] Kubo, Y., Iketomi, O., Nakashima, T., and Torii, K., Experimental Study of Fracture of Reinforced Steel Bar in Concrete Structures due to Alkali-Silica Expansion, ACI SP 212-40, 2003, 637-652.

[17] Sims, I., Alkali-Silica-Reaction – UK Experience, In Book "The Alkali-Silica Reaction in Concrete, Ed. Swamy, R.N., Blackie, Glasgow and London, U.K., New York, USA, 1990, 122-187.

[18] Mohammed, T.U., Hamada, H., and Yamaji, T., Alkali-Silica Reaction-Induced Strains over Concrete Surface and Steel Bars in Concrete, ACI Materials Journal, 2003, 100 (2), 133-142.

[19] Mohammed, T.U., and Hidenori, H., Relation between Strain on Surface and Strain over Embedded Steel Bars in ASR Affected Concrete Members, Journal of Advanced Concrete Technology, Japan Concrete Institute, 2003, 1 (1), 76-88.

* Tel. 81-46-844-5061, Fax. 81-46-844-0255, Email. tarek@pari.go.jp